(Article begins on next page)

Millimeter Wave Characterization of a Catadioptric Lens for Imaging Applications

Biddut Banik, *Student Member, IEEE*, Josip Vukusic, and Jan Stake, *Senior Member, IEEE*

***Abstract*— Characterization of a catadioptric dielectric lens-horn configuration for short-range sensing and imaging is presented. The focusing property is investigated both numerically and experimentally at 108 GHz. The lens-horn provides a focal spot of ~ 0.9λ at a distance of ~ 4.5λ. An imaging example employing the lens in a CW imaging setup is presented. A test pattern was imaged and a marked improvement in image resolution was observed. With the aid of the lens, features close to the wavelength are resolved, which are absent or indistinguishable otherwise.**

***Index Terms*— Dielectric loaded antennas, Lens antennas, Millimeter wave imaging, Shaped beam antennas, Terahertz imaging**

I. Introduction

Besides radio astronomy and remote sensing, the millimeter- and submillimeter-wave bands have found numerous "down to earth" applications [1] such as imaging, nondestructive testing, security screening and biomedical applications [2, 3]. In many imaging applications, the electromagnetic beam must be collimated and focused in order to attain a high resolution. For instance, far field imaging systems usually employ convex lenses, parabolic or elliptical mirrors, to create a focus point at a distance [4]. However, the maximum resolution of these systems is limited by the apertures and the distance. The well-known Abbe limit sets the ultimate spatial resolution to ~ λ/2 [5] and generally it is not possible to resolve objects less than few wavelengths [4]. Moreover, those systems pose complications towards compact and integrated solutions. On the other hand, nearfield imaging systems can resolve features much smaller than a wavelength [6]. However, for many practical applications, a short-range imaging and sensing system with a moderate spatial resolution is sufficient.

For short-range imaging and sensing systems, large numerical aperture lenses are conventionally used in order to achieve short focal length. Refractive lenses are required to have large diameter and therefore hinder compactness and integration. In this work, we propose a catadioptric lens configuration which provides an ultra-compact solution for short-range imaging systems while maintaining adequate resolution for many applications.

Manuscript received June 18, 2009. This work was supported by VINNOVA.

The authors are with the Physical Electronics Laboratory, Department of Microtechnology and Nanoscience, Chalmers University of Technology, SE-412 96 Göteborg, Sweden. (e-mail: biddut.banik@chalmers.se).

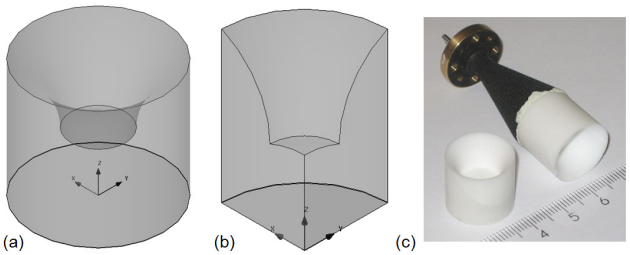

Fig. 1. (a) 3-D view of the catadioptric lens, (b) cross-sectional view, and (c) the fabricated 18 mm diameter catadioptric lens along with the lens-horn (WR-10 standard gain conical horn) configuration.

The catadioptric dielectric lens, shown in Fig. 1, provides an attractive solution as a focusing element. The lens and its focal length are electrically small (in the order of few wavelengths). Radiating elements and sensors can be physically coupled to the lens in order to achieve short-range focusing ability, therefore, enabling a compact system. Thus, the lens provides greater ease of system integration compared to the conventional quasioptical components.

The design and working principles of the catadioptric lens have already been reported [7, 8]. However, the current research concentrates on more extensive characterization of focusing properties and implementing the lens in millimeter wave imaging setups.

In this paper, we present simulation and experimental characterization results of a catadioptric lens at W band frequencies. The focusing property and the intensity profiles of the lens, fed by a WR-10 standard gain conical horn, have been investigated and results are presented. A metal pattern, having different sizes of holes, was used to inspect the spatial resolution of the setup. Finally, the lens was employed in a CW imaging setup and an example is presented.

II. Design and Analysis

The catadioptric lens consists of a hemispherical part with a "hornlike" extension on top of it, as shown in Fig. 1. This extended portion causes total internal reflection, which in turn creates the focus point [7]. An 18 mm diameter lens has been fabricated from MACOR ($\varepsilon_r = 5.6$), shown in Fig. 1. We have chosen 108 GHz (λ_0 = 2.78 mm) for characterization and measurement purposes due to the available source.

In contrast to analytical methods, a 3D EM FDTD solver package, CST Microwave Studio, has been used to analyze

the performance of the lens. Fig. 2 (a) shows the simulation setup of the catadioptric lens fed by a WR-10 conical horn. We have utilized symmetry-planes along E-plane and H-plane in order to reduce computational time and complexities. Perfectly matched layer boundaries were used, otherwise. The model in CST had 0.45 million meshcells. Fig. 2 (b) illustrates the simulated normalized intensity plot at 108 GHz along E-plane and H-plane where a focus region is observed. Fig. 2 (a) also shows the normalized intensity plot at the focal plane. At this frequency, the lens diameter D_{lens} is ~ 6.5 λ_0 or ~15 λ_{MACOR} where λ_0 is free space wavelength and λ_{MACOR} is the wavelength in MACOR.

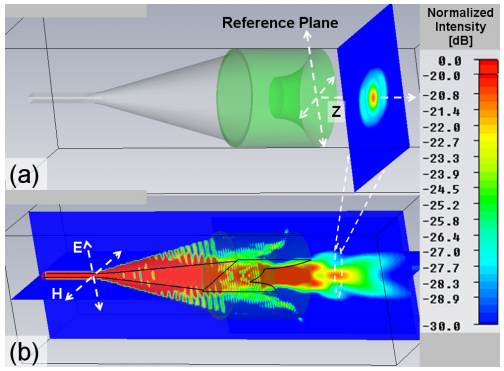

Fig. 2. (a) Simulation setup for the lens-horn configuration and intensity plot at the focal plane. (b) Simulated intensity plot along E-plane and H-plane. The simulation was performed at 108 GHz.

III. Characterization of the Lens

Fig. 3 shows the characterization and transmission measurement setup. The source consists of an Agilent E8257D PSG signal generator, a Spacek high power amplifier and a Heterostructure Barrier Varactor (HBV) tripler [9]. The source, set to 10 mW output power, was used to feed the lens, coupled via a conical standard gain horn (W-band). An open-ended rectangular waveguide probe, connected to an Erickson Power Meter (PM2), was used as the RF-detector. In order to reduce standing waves, a knife-edge profile for the waveguide probe was realized by thinning the sidewalls using a file. For nearfield mapping, the probe and the power meter were mounted on a computer-controlled 3-axis stage. In other cases, objects under investigation were mounted on the stage.

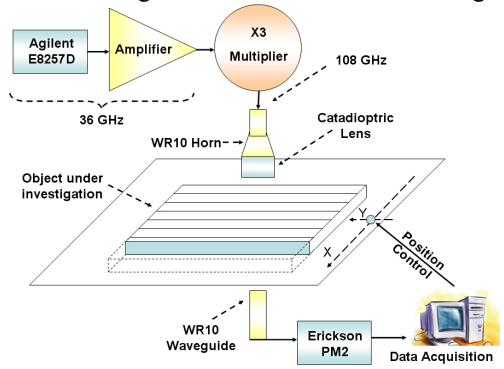

Fig. 3. Characterization and measurement setup.

Fig. 4 (a) shows the normalized intensity plot in dB at 108 GHz along Z axis attained by simulations and measurements. In order to account for the probe, simulations were also done placing a probe at different positions along Z axis and normalized S_{21} (in dB) is plotted. The measurements were done at 0.1 mm steps. Both the simulated and measured profiles indicate focus regions at Z ~ 3.5 mm and ~ 12 mm. However, from the practical application point of view, the foci at the farther points are more interesting. Moreover, the simulated intensity plot, shown in Fig. 2 (b), indicates that the second focus is more radially symmetric and well-defined. Fig. 4 (b) shows the simulated and measured lateral intensity profiles along E-plane and H-plane at Z = 12 mm. The figure indicates that the lens provides 3-dB spatial discrimination at ~ 2 mm or ~ 0.7λ_0. The agreement between measured and simulated intensity profiles is reasonable. The discrepancies can be attributed to the uncertainties of the material parameter (MACOR), horn model, lens-horn interface and to perturbation of the nearfield while using the probe.

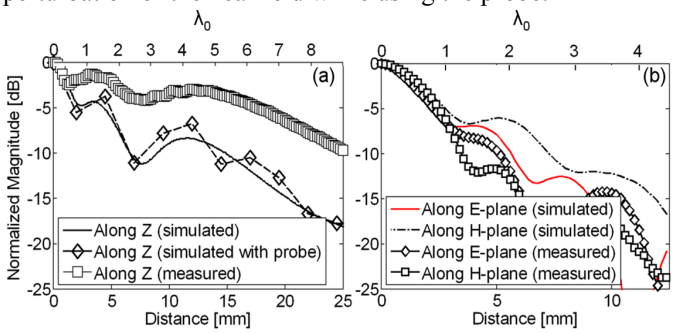

Fig. 4. Simulated and measured nearfield pattern at 108 GHz along (a) Z axis, and (b) E-plane and H-plane at Z = 12 mm.

In order to determine the focal diameter and the edge spread function (ESF) of the lens-horn, the edge of an aluminum screen was moved across the focus (Z = 12 mm). The 10%–90% rise in the transmitted power occurs over ~ 0.9λ_0, which provides a measure for the focal spot size [10]. Fig. 5 (a) shows the ESF. Line spread function (LSF) was derived from ESF, normalized, fitted to Gaussian distribution and σ = 0.4λ was obtained. Assuming rotational symmetry, point spread function (PSF) was constructed from LSF. Fig. 5 (b) shows the PSF.

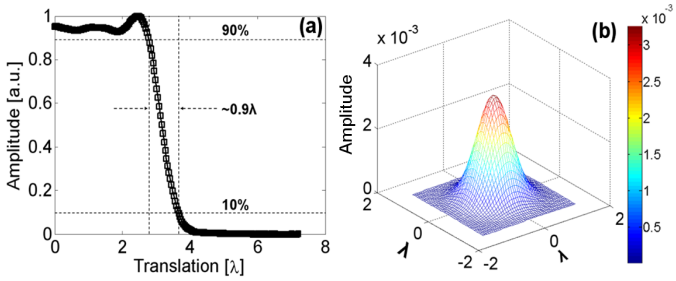

Fig. 5. (a) Edge spread function (ESF), and (b) point spread function (PSF).

In order to study the resolution, a metallic pattern was made having holes ranging from 1 mm to 3 mm with 0.25 mm steps. The holes are spaced at 5 mm from each other. Fig. 6 (a) shows the photograph of the metallic pattern. The pattern was imaged at 108 GHz using the setup illustrated in Fig. 3. Fig. 6 (b) shows the image of the pattern when only the horn was used as the transmitter while Fig. 6 (c) shows the image for lens-coupled horn transmitter. The images are of 121 × 121 pixels and represent the contrast in dB. The contrast is

defined as $(I-I_{min})/(I_{max}+I_{min})$ where I_{max} and I_{min} are the maximum and minimum intensities, consecutively. It can be observed from the figures that the lens-coupled system provides significantly improved and comprehensible images. Later, the image, shown in Fig. 6 (c), was deconvolved using the obtained PSF and the resulting image is shown in Fig. 6 (d). This deconvolved image closely resembles the optical image, shown in Fig. 6 (a).

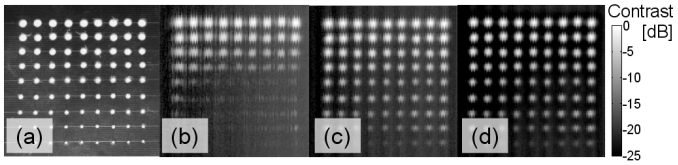

Fig. 6. (a) Metallic pattern having holes ranging from 1 mm to 3 mm with 0.25 mm steps. Images of the metallic pattern (b) without and (c) with the lens, and (d) shows the deconvolved image of (c). The images represent the contrast in dB.

Fig. 7 shows the contrast in dB and 3 dB-down points for a scan across the holes of different sizes of the metallic pattern, using lens-horn and only horn as transmitter. The figure indicates that due to the focusing of the lens, the *SNR* is increased making the smallest holes visible. Therefore, with the aid of the lens, features close a wavelength are resolved, which are absent or indistinguishable otherwise.

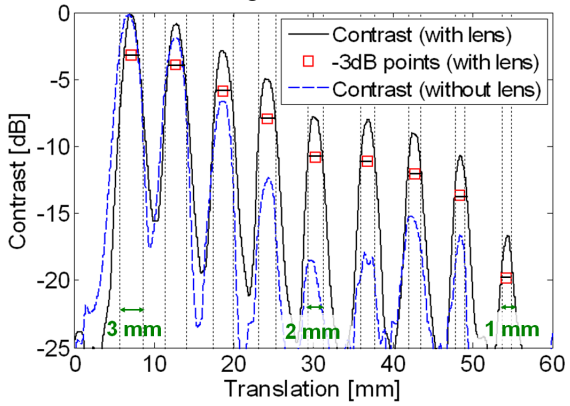

Fig. 7. Contrast in dB for a scan across the holes of different sizes (3 mm to 1 mm with 0.25 mm steps) of the metallic pattern with and without the lens.

IV. Imaging Examples

In this section, an imaging example at 108 GHz employing the catadioptric lens is presented. The transmission-mode CW imaging setup included lens-coupled horn transmitter and the waveguide probe was connected to a power meter, as shown in Fig. 3. The setup was used to image a partially dead leaf. Different parts of the leaf, e.g. veins, introduce different amounts of transmission losses which correspond to their water content. Fig. 8 (a) shows the photograph of the leaf where the dark colors correspond to the "living" parts and therefore indicates more water content. Fig. 8 (b) shows part of the leaf (6 cm × 6 cm), which was imaged while Fig. 8(c) shows the millimeter-wave image (121 × 121 pixels). Compared to the photograph, shown in Fig. 8 (b), the leaf veins and watery parts of the leaf are clearly distinguishable in Fig. 8 (c).

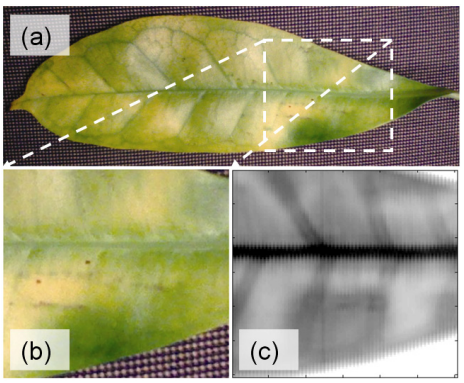

Fig. 8. (a) Photograph of the partially dead leaf (b) part of the leaf and (c) its scanned (raw) image at 108 GHz.

V. Conclusion

The focusing property of catadioptric lens is analyzed by FDTD. The characterization results of the lens show that, being electrically small, catadioptric lenses are suitable for compact and short-range imaging systems. The lens-horn provides a focal spot of ~ 0.9λ. A test pattern was used and significantly improved image was obtained. An imaging example has been presented employing the catadioptric lens. Our future investigation encompasses optimizing the lens-geometry for a certain intensity profile.

Acknowledgment

The authors thank Carl-Magnus Kihlman for machining the catadioptric lens. The authors are thankful to Wasa Millimeter Wave AB for providing the RF source. The authors would also thank Prof. Sheila Galt, Dr. Jörgen Bengtsson, and Dr. Sergey Cherednichenko for helpful discussions.

References

[1] P. H. Siegel, "Terahertz technology," *IEEE Transactions on Microwave Theory and Techniques*, vol. 50, pp. 910-928, 2002.

[2] E. Pickwell and V. P. Wallace, "Biomedical applications of terahertz technology," *Journal of Physics D: Applied Physics*, vol. 39, pp. 301-310, 2006.

[3] M. Tonouchi, "Cutting-edge terahertz technology," *Nat Photon*, vol. 1, pp. 97-105, 2007.

[4] R. Appleby and H. B. Wallace, "Standoff Detection of Weapons and Contraband in the 100 GHz to 1 THz Region," *IEEE Trans. Antennas Propag.*, vol. 55, pp. 2944-2956, 2007.

[5] E. Abbe, "Beiträge zur Theorie des Mikroskops und der mikroskopischen Wahrnehmung," *Archiv für Mikroskopische Anatomie*, vol. 9, pp. 413-418, 1873.

[6] B. T. Rosner and D. W. van der Weide, "High-frequency near-field microscopy," *Review of Scientific Instruments*, vol. 73, pp. 2505-2525, 2002.

[7] B. K. Banik, J. Vukusic, H. Merkel, and J. Stake, "A novel catadioptric dielectric lens for microwave and terahertz applications," *Microwave and Optical Technology Letters*, vol. 50, pp. 416-19, 2008.

[8] B. Banik, J. Vukusic, and J. Stake, "Catadioptric dielectric lens for imaging applications," *Proc. 33rd Intern. Conference on Infrared, Millimeter, and Terahertz Waves (IRMMW-THz), 2008*, pp. 1-2, 2008.

[9] J. Vukusic, T. Bryllert, T. A. Emadi, M. Sadeghi, and J. Stake, "A 0.2-W Heterostructure Barrier Varactor Frequency Tripler at 113 GHz," *Electron Device Letters, IEEE*, vol. 28, pp. 340-342, 2007.

[10] K. J. Siebert, H. Quast, R. Leonhardt, T. Loffler, M. Thomson, T. Bauer, H. G. Roskos, and S. Czasch, "Continuous-wave all-optoelectronic terahertz imaging," *Applied Physics Letters*, vol. 80, pp. 3003-3005, 2002.